

Universal properties of residual moments in heavy-fermion metals

Ewan Scott¹ and Michal Kwasigroch^{1,2}

¹*Department of Mathematics, University College London,
Gordon St., London WC1H 0AY, United Kingdom*

²*Trinity College, Cambridge, CB2 1TQ, United Kingdom*

(Dated: July 2, 2024)

We identify common features, seen across a wide range of actinide and lanthanide based heavy-fermion metals, that we associate with the universal properties of the residual moments generated by Kondo hybridisation. The features include the opposing anisotropies of the effective moments and Curie-Weiss constants, the reorientation of the magnetic easy axis, the hard-axis susceptibility maximum and the hard-axis metamagnetic transition. The extension of large- N Read-Newns theory to the underscreened Kondo lattice allows us to study large magnetic fluctuations of residual local moments in the presence of strong f - d hybridisation. We derive an effective Hamiltonian for the residual moments and show that competing single-ion and exchange anisotropies are responsible for the easy-axis reorientation. We identify a strong-coupling regime, where the temperature of the easy-axis reorientation is *directly proportional* to the coherence temperature and find good agreement across several Eu and U based heavy-fermion families, as well as a weak-coupling regime, where the easy axis flips just before the onset of magnetic order, as is seen in many Ce and Yb heavy-fermion compounds. We show that the exchange anisotropy of the residual moments can also generate a maximum in the hard-axis susceptibility, and find good agreement with UTe_2 at low pressures, suggesting that this material is particularly well described by the single-channel $S = 1$ model. Finally, we speculate on the possible pairing interactions generated by the fluctuations of the residual moments.

Introduction. – Heavy-fermion systems entwine electronic and magnetic degrees of freedom leading to a rich variety of phenomena such as high field superconductivity mediated by spin fluctuations [1–4], metamagnetic transitions [5], or the reorientation of the easy axis [6]. The interweaving begins with the formation of the flat heavy-fermion bands as the scattering of electrons from local magnetic moments becomes coherent. The emergent Fermi liquid excitations coexist with the residual local moments that form. Although many general questions remain, this ‘two-fluid’ picture is a useful perspective in which to view a number of experimental observations [7–10], as well as theoretical results [11–13], where Kondo hybridisation has been found to coexist with magnetic order. The emergent residual moments and quasi-particles originate from the same microscopic building blocks and therefore remain entwined. For example, anisotropy of the moments, that was initially of single-ion character, becomes non-local after heavy-fermion band formation, generating anisotropic magnetic fluctuations, and potentially, superconducting pairing.

The rich phenomenology of local-moment magnetism in heavy-fermion metals is generally sensitive to the underlying crystal structure, anisotropy, or valency of the local-moment ions. Nonetheless, across a wide range of lanthanide and actinide compounds some robust universal features emerge [4, 6, 14]. One example is the reorientation of the magnetic easy axis at low temperatures, that is strongly correlated with the presence of the coherence maximum in the material’s resistivity, as well as opposing anisotropies in the effective magnetic moments and Curie-Weiss constants.

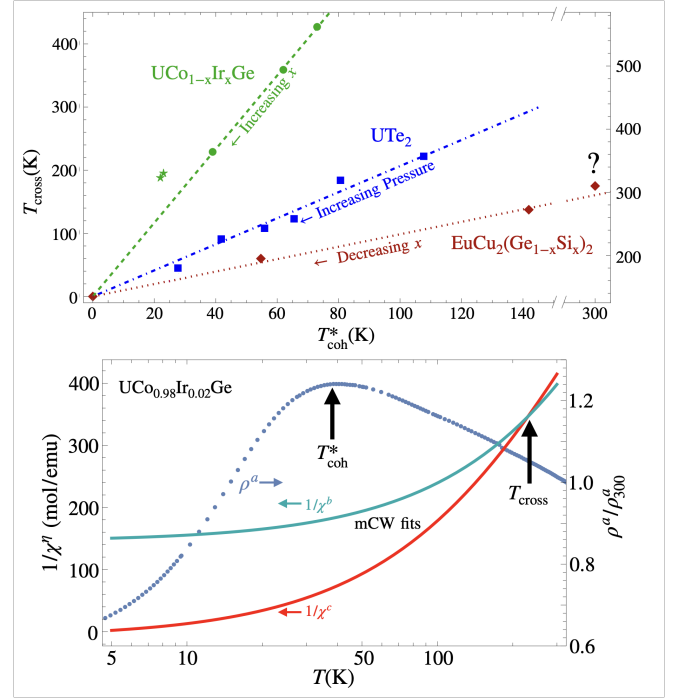


FIG. 1. Top: The easy-axis reorientation temperature, T_{cross} , against the coherence temperature (from the coherence maximum in the resistivity), T_{coh}^* , for three compounds: UTe_2 [15, 16], $\text{UCo}_{1-x}\text{Ir}_x\text{Ge}$ [17, 18], and $\text{EuCu}_2(\text{Ge}_{1-x}\text{Si}_x)_2$ [19]. The *direct proportionality* fits suggest that the same energy scale is responsible for the development of coherence and easy-axis reorientation. (For $\text{UCo}_{1-x}\text{Ir}_x\text{Ge}$, the fit does not include the stars, and for $\text{EuCu}_2(\text{Ge}_{1-x}\text{Si}_x)_2$ it does not include the highest T_{cross} , which is a tentative prediction.) Bottom: A plot of the a-axis resistivity and modified Curie-Weiss fits of b and c axis susceptibilities for $\text{UCo}_{0.98}\text{Ir}_{0.02}\text{Ge}$ showing T_{coh}^* and T_{cross} . A detailed description of all the plotted data and any extrapolations used can be found in Table I.

The reorientation of the easy axis is identified by a crossing of magnetic susceptibilities for fields along two perpendicular directions. This trend was first noticed in Ref. [6] across a wide range of Yb and Ce based Kondo ferromagnets, where the easy axis flips by 90 degrees just before the onset of magnetic order. Here, we widen the universality of this phenomenon by identifying Eu and U based heavy-fermion magnetic compounds, with multiple f -electrons per magnetic ion, that undergo easy-axis reorientation [15, 17, 19–24].

The universal features are not limited to the reorientation of the easy axis. In U and Eu based magnets we notice that the reorientation is often linked to the presence of a maximum in the temperature-dependence of the susceptibility along the axis which loses its ‘easy-axis status’ upon cooling [15, 17, 19–21, 24]. This hard-axis maximum is in turn connected to a metamagnetic transition when a high magnetic field is applied along the axis at lower temperatures [15, 17, 20, 24]. In fact, looking at all the compounds that we have surveyed, it appears that a metamagnetic transition in a high field applied along the hard axis implies a maximum in the the susceptibility along this axis at a higher temperature, which in turn implies that it becomes the easy axis at an even higher temperature.

Unlike in Ce or Yb based materials, in Eu or U based heavy-fermion compounds the reorientation of the easy axis can take place far away from the onset of magnetic order, or even in its absence. For example, UCoGe has a coherence maximum in the resistivity response along the b -axis at $T_{\text{coh}}^* = 170$ K, a Curie temperature of $T_C = 2.5$ K and a projected temperature of easy axis reorientation of $T_{\text{cross}} = 427$ K, obtained from modified Curie-Weiss (mCW) fits [25] for measurements up to 400 K [18]. (See the bottom panel of Fig. 1 for an example of T_{cross} obtained from mCW fits and T_{coh}^* from the coherence maximum in the resistivity.) Remarkably, we find that, in these compounds, the crossing and coherence temperatures appear to be *directly proportional*, showing that the same energy scale is responsible for both (see Fig. 1 (top), with a detailed description of all the plotted data given in Table I). The formation of the heavy fermion bands, which is responsible for T_{coh}^* and, we believe, for T_{cross} , takes place at a temperature much higher than the onset of magnetic order pointing to the underscreened nature of the underlying Kondo lattice and a regime where the Kondo energy, T_K , is much larger than the RKKY energy scale, T_{RKKY} , that is not captured by the usual Doniach argument [26].

Motivated by the above observation, we present a generalisation of the standard large- N Read-Newns theory to the underscreened Kondo lattice, that will allow us to study heavy-fermion magnetism in a regime, where $T_{\text{RKKY}} \ll T_K$. We present here the main results of our approach as well as experimental fits with the detailed derivations published elsewhere [27]. We focus on the underscreened $S = 1$ Kondo lattice with a single-ion anisotropy, as it already captures a wide range of

phenomena such as easy-axis reorientation, competing Curie-Weiss and effective moment anisotropies, and the maximum in the low temperature hard-axis susceptibility.

Model. – The underscreened $S = 1$ Kondo lattice with a generic single-ion anisotropy is described by the following Hamiltonian

$$H = J_K \sum_i \mathbf{S}(\mathbf{r}_i) \cdot \mathbf{s}(\mathbf{r}_i) + \sum_{\mathbf{k}\sigma} \epsilon_{\mathbf{k}} c_{\sigma}^{\dagger}(\mathbf{k}) c_{\sigma}(\mathbf{k}) + \sum_{\eta i} D^{\eta} (S^{\eta}(\mathbf{r}_i))^2, \quad (1)$$

where $J_K > 0$ is the Kondo coupling between local spin \mathbf{S}_i and the conduction electron spin \mathbf{s}_i . For simplicity, we have assumed that electrons and spins occupy the same Bravais lattice sites. $\epsilon_{\mathbf{k}}$ is the linearised conduction band in the vicinity of the Fermi surface such that $|\epsilon_{\mathbf{k}}| < \Lambda$. $D^{x,y,z}$ is a general single-ion anisotropy for spin-1 [28]. We will work away from the insulating limit, i.e., in the heavy Fermi liquid phase.

We write the $S = 1$ local moments in the Schwinger fermion representation [29, 30],

$$S^{\eta}(\mathbf{r}_i) = \sum_{a=1,2} S_a^{\eta}(\mathbf{r}_i) = \frac{1}{2} \sum_{a\sigma\sigma'} f_{a\sigma}^{\dagger}(\mathbf{r}_i) \sigma_{\sigma\sigma'}^{\eta} f_{a\sigma'}(\mathbf{r}_i), \quad (2)$$

where $a = 1, 2$ index the two spin-1/2 fermions, σ, σ' denote the up/down spin indices, $\sigma^{x,y,z}$ are Pauli matrices and $f_{a\sigma}(\mathbf{r}_i)$ obey the usual fermionic anticommutation relations. We will also promote the $SU(2)$ spin degrees of freedom to $SU(N)$. This can be done in a number of ways and we will choose to have $N/2$ replicas of spin-up states and an equal number of spin-down states on each lattice site, with half of them occupied, so that we are connected most straightforwardly to the physical $N = 2$ limit. N will be the control parameter for the large- N theory. The Hamiltonian can be written (up to a constant) as

$$H_N = \frac{J_K}{N} \sum_{a\alpha\sigma\beta\sigma' i} f_{a\alpha\sigma}^{\dagger}(\mathbf{r}_i) f_{a\beta\sigma'}(\mathbf{r}_i) c_{\beta\sigma'}^{\dagger}(\mathbf{r}_i) c_{\alpha\sigma}(\mathbf{r}_i) + \sum_{\mathbf{k}\alpha} \epsilon_{\mathbf{k}} c_{\alpha\sigma}^{\dagger}(\mathbf{k}) c_{\alpha\sigma}(\mathbf{k}) + \sum_{i,\alpha} D^{\eta} \left(\sum_a S_{a\alpha}^{\eta}(\mathbf{r}_i) \right)^2,$$

where

$$S_{a\alpha}^{\eta}(\mathbf{r}_i) = \sum_{\sigma\sigma'} f_{a\alpha\sigma}^{\dagger}(\mathbf{r}_i) \sigma_{\sigma\sigma'}^{\eta} f_{a\alpha\sigma'}(\mathbf{r}_i), \quad (3)$$

and α, β index the spin up/down replicas. We have rescaled the Kondo coupling $J_K \rightarrow (2J_K/N)$ so that energy density remains finite as $N \rightarrow \infty$, and $H_{N=2} = H$. The enlargement of the Hilbert space through the Schwinger fermion representation comes with several con-

straints and associated gauge symmetries:

$$\begin{aligned}\hat{n}_i^f &:= \sum_a \hat{n}_{ai}^f = \sum_{\alpha\sigma} f_{\alpha\sigma}^\dagger(\mathbf{r}_i) f_{\alpha\sigma}(\mathbf{r}_i) = N, \\ \hat{T}_i^\eta &:= \frac{1}{2} \sum_{aa'\alpha\sigma} f_{\alpha\sigma}^\dagger(\mathbf{r}_i) \tau_{aa'}^\eta f_{a'\alpha\sigma}(\mathbf{r}_i) = 0,\end{aligned}\quad (4)$$

where $\tau^{x,y,z}$ are again Pauli matrices, which now act on the 2-dimensional a subspace. We can understand the constraints \hat{n}_i^f and \hat{T}_i^η as together ensuring that there are $\hat{n}_{1i}^f = \frac{N}{2}$ f_1 -fermions and $\hat{n}_{2i}^f = \frac{N}{2}$ f_2 -fermions on each lattice site. The constraints $\hat{T}^{x,y}$ couple the $SU(N)$ f_1 and f_2 spins, which for $N = 2$ projects out the singlet state and corresponds to an infinite Hund's coupling between f_1 and f_2 moments. The constraints generate the $U(2) \sim U(1) \times SU(2)$ group of local gauge transformations.

The isotropic ($D^\eta = 0$) system is controlled by the fixed-gauge saddle point as $N \rightarrow \infty$. Read-Newns large- N theory introduces the hybridisation field

$$\begin{pmatrix} \hat{V}_{1i} \\ \hat{V}_{2i} \end{pmatrix} = \frac{1}{N} \sum_{\alpha\sigma} \begin{pmatrix} f_{1\alpha\sigma}^\dagger(\mathbf{r}_i) c_{\alpha\sigma}(\mathbf{r}_i) \\ f_{2\alpha\sigma}^\dagger(\mathbf{r}_i) c_{\alpha\sigma}(\mathbf{r}_i) \end{pmatrix}, \quad (5)$$

and the $U(2)$ gauge symmetry can be used to set $\hat{V}_{2i} = 0$ and $\hat{V}_{1i} > 0$. We emphasise that this is not done just on the level of expectation values. Quantum fluctuations (in imaginary time) of \hat{V}_{2i} are also quenched. f_2 -fermions are thus decoupled from the conduction electrons in the hybridisation channel. The constraint-enforcing gauge fields develop a non-zero stiffness softening the constraints on \hat{n}_{1i}^f and \hat{T}_i^η . A residual $U(1)$ gauge symmetry remains so that the constraint on \hat{n}_{2i}^f is still enforced exactly.

The fluctuations of the constraint-enforcing gauge fields around the saddle point generate the following interactions

$$\begin{aligned}\Delta H_{\text{fluc.}} &= G_{\lambda\lambda}(0) \sum_i \left(\hat{n}_{1i}^f - \frac{N}{2} \right)^2 + \\ &+ G_{\phi^\dagger\phi}(0) \sum_{i,\alpha\sigma\beta\sigma'} f_{1\alpha\sigma}^\dagger(\mathbf{r}_i) f_{1\beta\sigma'}(\mathbf{r}_i) f_{2\beta\sigma'}^\dagger(\mathbf{r}_i) f_{2\alpha\sigma}(\mathbf{r}_i),\end{aligned}\quad (6)$$

where the gauge-field Green's functions in the low-energy limit scale as $G_{\lambda\lambda}(0) \sim T_K/N$ and $G_{\phi^\dagger\phi}(0) \sim T_K(N \log(T/T_K))^{-1} < 0$ [31]. The infinite Hubbard-like interaction that enforced the constraint on \hat{n}_{1i}^f has been renormalised to a finite interaction and so has the infinite Hund-like interaction that enforced the constraint on $\hat{T}_i^{x,y}$. The latter is the residual ferromagnetic interaction between the unscreened f_2 -moments and the heavy fermions (f_1 -fermions are now part of the heavy fermion quasiparticle). The stiffness of the gauge-field whose fluctuations generate the Hund-like interaction diverges logarithmically in the zero-temperature limit leading to logarithmically decaying residual ferromagnetic interaction. This agrees with the results for a single impurity [32, 33].

While it is true that fractional violations of the constraints $\frac{1}{N} \langle (\hat{T}^\eta)^2 \rangle^{1/2} \sim 1/\sqrt{N}$ are small for large- N , it is remarkable that the $N = \infty$ saddle point can capture the behaviour of physical systems with $N = 2$, and that it has even provided quantitative agreement in many cases [34]. Intuitively, the system flows to the large- N fixed point in the RG sense. The long-range coherence of the hybridisation field allows for the averaging over close-by (in imaginary time and real space) hybridisation fields, and effectively a local hybridisation process is coupled to the average of many surrounding ones. In many ways, this is what the introduction of additional fictitious spin flavours is equivalent to.

Residual local moments. – The unhybridised f_2 -moments thus decouple in the zero-temperature limit as the residual ferromagnetic interaction decays logarithmically to zero. This would be the complete story for a single impurity, but for a Kondo lattice, the macroscopic degeneracy of the f_2 -moment subspace can be broken by a coupling that leaves a vanishing imprint on the f_1 - c heavy fermion subspace. Because of the $U(2)$ gauge symmetry, the f_2 -fermions can be decoupled from the conduction electrons in the hybridisation channel but not the magnetic channel since magnetisation, $S^\eta(\mathbf{r}_i)$, is a gauge-invariant physical operator. Unfortunately, the fixed-gauge saddle point expansion (up to first order in $1/N$) does not include interactions in this channel and the Kondo-hybridised phase is stable against RKKY magnetism. However, the fact that for any finite N , as $J_K\rho \rightarrow 0$, the conventional RKKY ground state becomes favourable over the Kondo-hybridised phase can be picked up variationally and this is indeed the original Doniach argument [35].

Motivated by the above observation, we consider the following variational ansatz for the state of the system at $T \ll T_K$

$$|\Psi\rangle = \prod_{\mathbf{k}\alpha\nu} \left(u_{\mathbf{k}\alpha\sigma}^\nu c_{\mathbf{k}\alpha\sigma}^\dagger + v_{\mathbf{k}\alpha\sigma}^\nu f_{1\mathbf{k}\alpha\sigma}^\dagger \right) |0\rangle \otimes \prod_i |\psi_{2i}\rangle, \quad (7)$$

where ν indexes two heavy fermion bands and $|\psi_{2i}\rangle$ is the state of the i -th f_2 -moment. By employing the usual static approximation for the f_2 -moments, calculating $\langle \Psi | H_N | \Psi \rangle$ with $\{u_{\mathbf{k}\alpha\sigma}^\nu, v_{\mathbf{k}\alpha\sigma}^\nu\}$ chosen to minimise the expectation value, we can derive the effective RKKY interaction between f_2 -moments that is mediated by the heavy fermions. Expanding to quadratic order in $1/N$ and D^η and linear order in an external magnetic field h , we obtain

$$H_{\text{eff}} = -\frac{1}{2} \sum_{\mathbf{q}\alpha\eta} \mathcal{J}^\eta(\mathbf{q}) S_{2\alpha}^\eta(\mathbf{q}) S_{2\alpha}^\eta(-\mathbf{q}) - \sqrt{N_s} \sum_{\eta\alpha} \tilde{h}^\eta S_{2\alpha}^\eta(\mathbf{0}), \quad (8)$$

where

$$\begin{aligned} \mathcal{J}^\eta(\mathbf{q}) &= \frac{4J_K^2}{N^2} \chi_{ee}(\mathbf{q}) + \frac{8J_K}{N} D^\eta \chi_{fe}(\mathbf{q}) + (2D^\eta)^2 \chi_{ff}(\mathbf{q}), \\ \tilde{h}^\eta &= 1 - \frac{2J_K}{N} (\chi_{ee}(\mathbf{0}) + \chi_{fe}(\mathbf{0})) - 2D^\eta (\chi_{ff}(\mathbf{0}) + \chi_{fe}(\mathbf{0})). \end{aligned} \quad (9)$$

The susceptibilities of the spin-1/2 Kondo lattice $N = \infty$ ground state are given by

$$\begin{aligned} \chi_{ee}(\mathbf{q}) &= \frac{1}{2N_s} \sum_{\mathbf{k}, \nu, \nu'} |u_{\mathbf{k}}^{\nu'}|^2 |u_{\mathbf{k}+\mathbf{q}}^{\nu'}| \frac{n(E_{\mathbf{k}+\mathbf{q}}^{\nu'}) - n(E_{\mathbf{k}}^{\nu})}{E_{\mathbf{k}}^{\nu} - E_{\mathbf{k}+\mathbf{q}}^{\nu'}}, \\ \chi_{fe}(\mathbf{q}) &= \frac{1}{2N_s} \sum_{\mathbf{k}, \nu, \nu'} \bar{v}_{\mathbf{k}}^{\nu} v_{\mathbf{k}+\mathbf{q}}^{\nu'} u_{\mathbf{k}}^{\nu} \bar{u}_{\mathbf{k}+\mathbf{q}}^{\nu'} \frac{n(E_{\mathbf{k}+\mathbf{q}}^{\nu'}) - n(E_{\mathbf{k}}^{\nu})}{E_{\mathbf{k}}^{\nu} - E_{\mathbf{k}+\mathbf{q}}^{\nu'}}, \\ \chi_{ff}(\mathbf{q}) &= \frac{1}{2N_s} \sum_{\mathbf{k}, \nu, \nu'} |v_{\mathbf{k}}^{\nu'}|^2 |v_{\mathbf{k}+\mathbf{q}}^{\nu'}| \frac{n(E_{\mathbf{k}+\mathbf{q}}^{\nu'}) - n(E_{\mathbf{k}}^{\nu})}{E_{\mathbf{k}}^{\nu} - E_{\mathbf{k}+\mathbf{q}}^{\nu'}}, \end{aligned} \quad (10)$$

where $\chi_{ee}(\mathbf{q})$ ($\chi_{fe}(\mathbf{q})$) gives the magnetic susceptibility of the conduction electrons (spin-1/2 local moments) when a \mathbf{q} -modulated magnetic field is applied isothermally to conduction electrons only. Similarly, $\chi_{ff}(\mathbf{q})$ gives the magnetic susceptibility of the spin-1/2 local moments, when the applied field only couples to them.

The effective Hamiltonian in Eq. 8 is the main result of our work and in the isotropic and insulating limit agrees with the Hamiltonian derived in Ref. [30] via a slightly different approach. There, the difference between $H_{N=2}$ and mean-field Hamiltonian (exact for $N = \infty$) was considered as the residual perturbative interaction and the effective Hamiltonian for the f_2 -subspace was obtained. They showed that the results of this approach agreed well with DMRG calculations for a 1D Kondo lattice problem.

Easy-axis reorientation. – Since $\chi(\mathbf{0})$ are all positive [27], the anisotropy of the effective field, \tilde{h}^η , and the anisotropy of the ferromagnetic exchange $\mathcal{J}(\mathbf{0})$ are of opposite sign to first order in D^η . Hard-axis anisotropy $D^\eta > 0$ leads to a reduction of the residual effective moment but a reinforcement of RKKY exchange between the residual moments along that direction. In particular, a ground state with FM order would have moments along the direction with the the highest D^η , and hence greatest ferromagnetic exchange but smallest susceptibility at high temperature in the free-moment regime – this is the hard-direction ordering discussed in Ref. [27, 45]. The single-ion and exchange anisotropies respectively correspond to the anisotropy in the effective moments μ_{eff}^η and Curie-Weiss constants Θ_{CW}^η . Indeed, in agreement with H_{eff} , many of the compounds surveyed have $(\Delta\mu_{\text{eff}}^\eta)/\mu_{\text{eff}} \sim -(\Delta\Theta_{\text{eff}}^\eta)/T_{\text{cross}}$, where Δ takes the difference between the two directions involved in the easy-axis reorientation and μ_{eff} is the average effective moment for these two directions. The competition between the two anisotropies leads to a reorientation of the easy axis at a

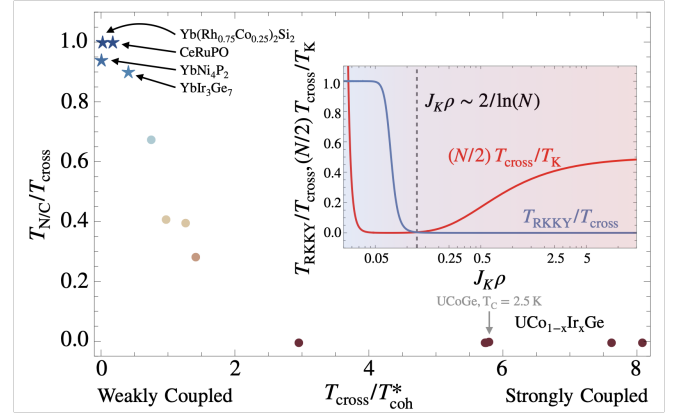


FIG. 2. The ratios $T_{N/C}/T_{\text{cross}}$ and $T_{\text{cross}}/T_{\text{coh}}^*$ plotted for several compounds. Yb and Ce compounds [6, 36–44] are in the weak coupling regime and $\text{UCo}_{1-x}\text{Ir}_x\text{Ge}$ transitions between regimes with x . Inset: the ratios $T_{\text{RKKY}}/T_{\text{cross}}$ and $(N/2)T_{\text{cross}}/T_K$ plotted against the Kondo coupling strength, $J_K\rho$. There are two regimes: Weak coupling, $T_{\text{RKKY}}/T_{\text{cross}} \sim 1$, and strong coupling, $(N/2)T_{\text{cross}}/T_K > 0$. The divergence of the red curve signals a return to the conventional RKKY phase when $T_{\text{RKKY}} \gtrsim T_K$.

temperature of

$$\begin{aligned} T_{\text{cross}} &= \frac{2J_K}{N} \frac{\chi_{fe}(\mathbf{0})}{\chi_{ff}(\mathbf{0}) + \chi_{fe}(\mathbf{0})} \\ &+ \frac{J_K^2}{N^2} \left(\chi_{ee}(\mathbf{0}) - \frac{\chi_{fe}(\mathbf{0})(\chi_{ee}(\mathbf{0}) + \chi_{fe}(\mathbf{0}))}{\chi_{ff}(\mathbf{0}) + \chi_{fe}(\mathbf{0})} \right), \end{aligned} \quad (11)$$

to quadratic order in $1/N$ and first non-vanishing order in D^η . We identify two limits as depicted in Fig. 2. In the strong-coupling limit $J_K\rho \gg 1$ (this corresponds to $NJ\rho \gg 1$), we have to first non-vanishing order in D^η and $1/N$

$$T_{\text{cross}} = \frac{J_K}{4N} = \frac{T_K}{N}, \quad (12)$$

where T_K is Kondo energy scale [46]. In the weak-coupling limit, for any fixed N , as $J_K\rho \rightarrow 0$, the crossing temperature tends to $T_{\text{RKKY}} = (J_K/N)^2 \chi_{ee}(\mathbf{0})$, the temperature at which FM order [47] sets in, before vanishing entirely, when $T_{\text{RKKY}} \gtrsim T_K$, the hybridisation field collapses and we have a conventional RKKY phase with no easy-axis reorientation. Fig. 2 illustrates the two regimes for both theory and the corresponding ratios experimentally measured for a range of compounds. It is found that $\text{UCo}_{1-x}\text{Ir}_x\text{Ge}$ spans the range from strongly coupled ($T_{N/C}/T_{\text{cross}} \sim 0$) to weakly coupled ($T_{N/C}/T_{\text{cross}} \sim 1$) as a function of the doping x , where $T_{N/C}$ is the Neel or Curie temperature depending on the type of magnetic order. On the other hand, the Ce and Yb compounds tend to lie in the weakly coupled regime, presumably because they are described by the fully compensated Coqblin-Schrieffer model and the residual moments vanish when $T_K \gg T_{\text{RKKY}}$.

If we extrapolate the strong-coupling large- N result to the physical case $N = 2$, we find that the crossing tem-

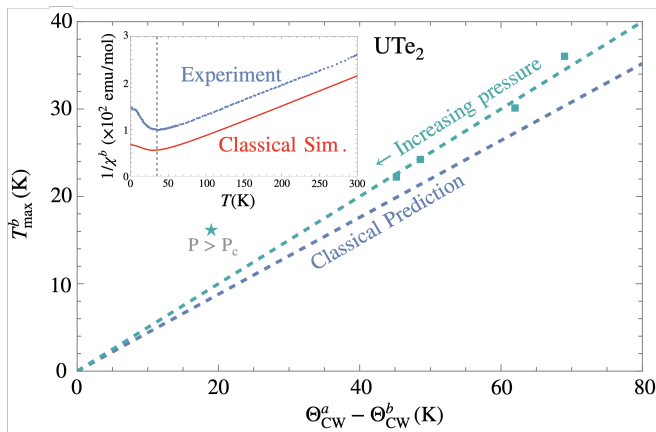


FIG. 3. The temperature of the b-axis maximum, T_{\max}^b , in UTe_2 against the difference in the Curie-Weiss constants $\Theta_{\text{CW}}^a - \Theta_{\text{CW}}^b$. The *direct proportionality* fit, which does not include the point above critical pressure with AFM order in the ground state, shows that the exchange anisotropy is the energy scale that is responsible for T_{\max}^b at low pressures. The fit has $T_{\max}^b \approx 0.5(\Theta_{\text{CW}}^a - \Theta_{\text{CW}}^b)$, close to the single-mode classical prediction of $T_{\max}^b \approx 0.44(\Theta_{\text{CW}}^a - \Theta_{\text{CW}}^b)$. The inset shows the single-mode classical simulation and experimental data at ambient pressure cited in the acknowledgements.

perature is proportional to the strength of the Kondo interaction, i.e. we should have $T_{\text{cross}} \propto T_{\text{coh}}^*$, which indeed shows excellent agreement with experimental data collected across a wide range of heavy-fermion compounds as shown in Fig. 1, where the Kondo coherence temperature is varied with pressure or doping for three heavy fermion compounds and is plotted against the easy-axis reorientation temperature, T_{cross} .

The above model would suggest that the axis with the lowest high-temperature susceptibility (highest D^η) should always become the low-temperature easy axis. This is rarely seen in orthorhombic systems (it has been seen in YbRhSb [48] at high pressures). In most compounds only the two highest susceptibilities cross with the third one always remaining quenched. We suggest that in those cases the anisotropy D^η of the axis with the lowest susceptibility is too large for the Kondo-hybridisation mechanism to overcome. In fact, it usually has the lowest effective moment as well as the lowest Curie-Weiss constant, which suggests that the mechanism is not in play. H_{eff} is only valid for $D^\eta \ll T_K$, but if we ramp up the anisotropy and look at the optimised variational wavefunction, the hybridisation field that is responsible for the reduction of the effective moment and the reinforcement of the Curie-Weiss constant eventually collapses and we revert to free moment behaviour, where the higher the D^η , the lower the susceptibility. This happens before the hybridisation field collapses for the two directions with lower D^η . We note that, although the collapse signals the return of the free-moment state, it is beyond the validity of our perturbative model.

Maximum in the hard-axis susceptibility. – A common

observation in heavy-fermion compounds is the presence of a maximum in the temperature dependence of the susceptibility along the low temperature hard axis (high temperature easy axis)[15]. The maximum is followed by a low-temperature region where $(\frac{\partial M}{\partial T})_h = -(\frac{\partial S}{\partial h})_T < 0$. Such a maximum appears to be a necessary, but not sufficient, prerequisite for a metamagnetic transition when a large field is applied along the low temperature hard axis at even lower temperatures [5, 49]. Here we argue that the anisotropy in the exchange that is responsible for the reorientation of the easy axis is also responsible for the maximum in the hard-axis susceptibility. By the fluctuation-dissipation theorem, the uniform susceptibility is a measure of the $\mathbf{q} = \mathbf{0}$ fluctuations along a given axis $\chi^\eta = \int_0^\beta \langle S_2^\eta(\mathbf{0}, \tau) S_2^\eta(\mathbf{0}, 0) \rangle_{H_{\text{eff}}} d\tau$. The cost of such fluctuations is lower along the easy axis than the hard axis and can lead to a quenching of the hard-axis fluctuations and susceptibility at a characteristic temperature that is of the order of the energy difference between spins aligned along the easy axis and spins aligned along the hard axis.

The quenching of the susceptibility can be captured by a single-mode classical simulation and we will focus on the case of UTe_2 at different pressures. We assume that the spins are confined to the ab -plane because of strong anisotropy along the c -direction (the c -axis susceptibility is significantly lower in the relevant temperature range). The corresponding classical Hamiltonian for spin- S is given by

$$H_{\text{cl}} = -2S(S+1)\Delta\Theta_{\text{CW}}\sin^2\theta - \tilde{h}^b S \cos\theta, \quad (13)$$

where $S = 1/2$, only Goldstone $\mathbf{q} = \mathbf{0}$ fluctuations were included and θ is the angle of the moment from the hard b -axis (field axis) towards the easy a -axis. The temperature of the susceptibility maximum is found to be $T_{\max}^b \approx 0.44(\Theta_{\text{CW}}^a - \Theta_{\text{CW}}^b)$, which is not far from the experimentally observed trend $T_{\max}^b \approx 0.5(\Theta_{\text{CW}}^a - \Theta_{\text{CW}}^b)$, as shown in Fig. 3. (In the classical simulation, the effective field \tilde{h}^b was chosen to recover the high-temperature behaviour.) The *direct proportionality* implies that exchange anisotropy is the energy scale that is responsible for T_{\max}^b . We note that the single-mode classical simulation underestimates the CW constant because AFM fluctuations are not included. This is presumably also why T_{\max}^b for $p > p_c$ (where AFM order sets in the ground state) departs from the *direct proportionality* trend.

The relatively good agreement with the classical $S = 1/2$ simulation adds to the growing evidence that that far above the coherence temperature the local moments in UTe_2 are $S = 1, L = 0$ and, following Kondo-hybridisation, the residual moments are $S = 1/2, L = 0$. Indeed, UTe_2 has been argued to have a $5f^2$ valency [50] and most recent measurements show the effective moment to be approximately $2.8\mu_B$ [51], which is close to that of a free $S = 1, L = 0$ moment. The saturation magnetisation per f.u. of $1\mu_B$ at low temperatures

points to a spin-1/2 residual moment and a single screening channel. The situation in UTe_2 should be compared with $\text{EuCu}_2(\text{Ge}_{1-x}\text{Si}_x)_2$, where the local moments are believed to be $S = 7/2, L = 0$ [19].

Spin-fluctuation mediated pairing interactions. –

Finally, we speculate on the possible pairing interactions of the heavy fermions that could be mediated by the low-energy fluctuations of the residual moments. In particular, we find a pairing interaction along the η -axis between f_1 and c fermions, which are now both part of the heavy-fermion quasiparticle,

$$H_{\text{pair}}^\eta = -\frac{J_K}{N} \sum_{ij\eta\alpha\sigma} D^\eta \chi_{ij}^\eta \left(f_{\alpha\sigma}^\dagger(\mathbf{r}_i) c_{\alpha\sigma}^\dagger(\mathbf{r}_j) c_{\alpha\sigma}(\mathbf{r}_j) f_{\alpha\sigma}(\mathbf{r}_i) - f_{\alpha\sigma}^\dagger(\mathbf{r}_i) c_{\alpha\bar{\sigma}}^\dagger(\mathbf{r}_j) c_{\alpha\bar{\sigma}}(\mathbf{r}_j) f_{\alpha\sigma}(\mathbf{r}_i) \right) \quad (14)$$

where the up/down fermionic spins are with respect to the η -axis and $\chi_{ij}^\eta = \int_0^\beta \langle S_{2\alpha}^\eta(\mathbf{r}_i, \tau) S_{2\alpha}^\eta(\mathbf{r}_j, 0) \rangle_{H_{\text{eff}}} d\tau$ is the susceptibility of the residual f_2 -moments. The above interaction leads to the intriguing possibility of the pairing channel being dependent on the sign of D^η . One might envisage a situation, where fluctuations of the residual moments generate triplet pairing along the low-temperature easy axis ($D^\eta > 0$), whereas fluctuations of the residual moments generate singlet pairing along the low-temperature hard axis ($D^\eta < 0$). This could potentially be the scenario found in UTe_2 for the a and b axes respectively.

Conclusion. – In summary, we have highlighted universal behaviours in heavy-fermion systems irrespective

of the compound's individual properties such as the valency or crystal structure. We propose a large- N theory which we demonstrate captures the physics of these heavy-fermion systems. We identify two regimes. When $T_{N/C}/T_{\text{cross}} \sim 1$ the reorientation of the easy axis occurs at the onset of magnetic order and the system is in the weak-coupling regime. The strong-coupling regime is characterised by $T_{\text{cross}} \propto T_{\text{coh}}^*$. Many of the uranium and europium compounds which we argue are in the strong-coupling regime exhibit a hierarchy of decreasing energy scales: the coherence temperature T_{coh}^* and the temperature of easy-axis reorientation T_{cross} ; the temperature of the hard-axis maximum $T_{\text{max}}^{\text{hard}}$; the metamagnetic transition in applied field along the hard-axis; and superconductivity.

We show that the easy-axis reorientation is caused by competing anisotropy in the exchange and effective moment. Further, we demonstrate that the exchange anisotropy can explain the maximum in the low temperature hard axis susceptibility. A classical Hamiltonian that captures this maximum was derived and agrees well with the experimental data.

Acknowledgments – We acknowledge the following people for providing experimental data on $\text{UCo}_{1-x}\text{Ir}_x\text{Ge}$ and $\text{URh}_{1-x}\text{Ir}_x\text{Ge}$: V. Sechovský, D. Hovančík, and J. Pospíšil and F. Malte Grosche, A. Eaton, Z. Wu for providing experimental data on UTe_2 . As well as those already mentioned, we would like to thank the following people for stimulating discussions: P. Coleman, C. Batista, M. Zhitomirsky, J. Annett, D. Adroja, F. Krüger, H. Hu, K. Wojcik, and G. Lonzarich for many imaginative ideas.

-
- [1] W. Knafo, M. Nardone, M. Vališka, A. Zitouni, G. Laperot, D. Aoki, G. Knebel, and D. Braithwaite, *Communications Physics* **4** (2021).
- [2] S. K. Lewin, C. E. Frank, S. Ran, J. Paglione, and N. P. Butch, *Reports on Progress in Physics* **86**, 114501 (2023).
- [3] D. Aoki, J.-P. Brison, J. Flouquet, K. Ishida, G. Knebel, Y. Tokunaga, and Y. Yanase, *Journal of Physics: Condensed Matter* **34**, 243002 (2022).
- [4] D. Aoki, K. Ishida, and J. Flouquet, *Journal of the Physical Society of Japan* **88**, 022001 (2019).
- [5] A. Miyake, Y. Shimizu, Y. J. Sato, D. Li, A. Nakamura, Y. Homma, F. Honda, J. Flouquet, M. Tokunaga, and D. Aoki, *Journal of the Physical Society of Japan* **88**, 063706 (2019).
- [6] D. Hafner, B. K. Rai, J. Banda, K. Kliemt, C. Krellner, J. Sichelschmidt, E. Morosan, C. Geibel, and M. Brando, *Phys. Rev. B* **99**, 201109 (2019).
- [7] Y.-f. Yang, Z. Fisk, H.-O. Lee, J. D. Thompson, and D. Pines, *Nature* **454**, 611 (2008).
- [8] G. Lonzarich, D. Pines, and Y. feng Yang, *Reports on Progress in Physics* **80**, 024501 (2016).
- [9] G. Lonzarich, D. Pines, and Y. feng Yang, *Reports on Progress in Physics* **80**, 024501 (2016).
- [10] X. Ji, X. Luo, Q. Chen, W. Feng, Q. Hao, Q. Liu, Y. Zhang, Y. Liu, X. Wang, S. Tan, and X. Lai, *Phys. Rev. B* **106**, 125120 (2022).
- [11] A. Gleis, S.-S. B. Lee, G. Kotliar, and J. von Delft, (2023), arXiv:2310.12672.
- [12] M. Raczkowski and F. F. Assaad, *Phys. Rev. Res.* **2**, 013276 (2020).
- [13] N. B. Perkins, M. D. Núñez Regueiro, B. Coqblin, and J. R. Iglesias, *Phys. Rev. B* **76**, 125101 (2007).
- [14] Y. Ōnuki, M. Hedo, and F. Honda, *Journal of the Physical Society of Japan* **89**, 102001 (2020).
- [15] D. Li, A. Nakamura, F. Honda, Y. Sato, Y. Homma, Y. Shimizu, J. Ishizuka, Y. Yanase, G. Knebel, J. Flouquet, and D. Aoki, *Journal of the Physical Society of Japan* **90** (2021).
- [16] M. O. Ajeesh, J. D. Thompson, E. D. Bauer, F. Ronning, S. M. Thomas, and P. F. S. Rosa, *Journal of the Physical Society of Japan* **93**, 055001 (2024).
- [17] D. Hovančík, A. Koriki, A. c. v. Bendová, P. Doležal, P. Proschek, M. Míšek, M. Reiffers, J. Prokleška, J. c. v. Pospíšil, and V. Sechovský, *Phys. Rev. B* **105**, 014436 (2022).
- [18] W. M. H. M. R. Troć, R. Wawryk and M. Samsel-

- Czekała, *Philosophical Magazine* **90**, 2249 (2010).
- [19] W. Iha, T. Yara, Y. Ashitomi, M. Kakihana, T. Takeuchi, F. Honda, A. Nakamura, D. Aoki, J. Gouchi, Y. Uwatoko, T. Kida, T. Tahara, M. Hagiwara, Y. Haga, M. Hedo, T. Nakama, and Y. Ōnuki, *Journal of the Physical Society of Japan* **87**, 064706 (2018).
- [20] J. c. v. Pospíšil, Y. Haga, S. Kambe, Y. Tokunaga, N. Tateiwa, D. Aoki, F. Honda, A. Nakamura, Y. Homma, E. Yamamoto, and T. Yamamura, *Phys. Rev. B* **95**, 155138 (2017).
- [21] M. Szlawska, M. Majewicz, D. Kowalska, and D. Kaczorowski, *Scientific Reports* **13** (2023).
- [22] M. Bleckmann, A. Otop, S. Süllow, R. Feyerherm, J. Klenke, A. Loose, R. Hendrikx, J. Mydosh, and H. Amitsuka, *Journal of Magnetism and Magnetic Materials* **322**, 2447 (2010).
- [23] J. Valenta, F. Honda, M. Vališka, P. Opletal, J. Kaštil, M. Míšek, M. Diviš, L. Sandratskii, J. Prchal, and V. Sechovský, *Phys. Rev. B* **97**, 144423 (2018).
- [24] Y. Hiranaka, A. Nakamura, M. Hedo, T. Takeuchi, A. Mori, Y. Hirose, K. Mitamura, K. Sugiyama, M. Hagiwara, T. Nakama, and Y. Ōnuki, *Journal of the Physical Society of Japan* **82**, 083708 (2013).
- [25] A mCW fit simply involves adding a constant offset to the usual Curie-Weiss susceptibility.
- [26] N. Read, D. M. Newns, and S. Doniach, *Phys. Rev. B* **30**, 3841 (1984).
- [27] E. Scott and M. Kwasigroch, In preparation.
- [28] Of course one of the D^7 can always be set to 0.
- [29] N. B. Perkins, M. D. Núñez Regueiro, B. Coqblin, and J. R. Iglesias, *Phys. Rev. B* **76**, 125101 (2007).
- [30] W.-H. Ko, H.-C. Jiang, J. G. Rau, and L. Balents, *Phys. Rev. B* **87**, 205107 (2013).
- [31] We note that the residual Hund-like interaction does not decay logarithmically but tends to a constant in the insulating half-filling limit.
- [32] Nozières, Ph. and Blandin, A., *J. Phys. France* **41**, 193 (1980).
- [33] A. Allerdt, R. Žitko, and A. E. Feiguin, *Phys. Rev. B* **97**, 045103 (2018).
- [34] P. Coleman and N. Andrei, *Journal of Physics C: Solid State Physics* **19**, 3211 (1986).
- [35] S. Doniach, *Physica B+C* **91**, 231 (1977).
- [36] C. Krellner, S. Lausberg, A. Steppke, M. Brando, L. Pedrero, H. Pfau, S. Tencé, H. Rosner, F. Steglich, and C. Geibel, *New Journal of Physics* **13**, 103014 (2011).
- [37] A. Steppke, R. KÜchler, S. Lausberg, E. Lengyel, L. Steinke, R. Borth, T. Lühmann, C. Krellner, M. Nicklas, C. Geibel, F. Steglich, and M. Brando, *Science* **339**, 933 (2013).
- [38] C. Krellner and C. Geibel, *Journal of Crystal Growth* **310**, 1875 (2008).
- [39] C. Krellner, N. S. Kini, E. M. Brüning, K. Koch, H. Rosner, M. Nicklas, M. Baenitz, and C. Geibel, *Phys. Rev. B* **76**, 104418 (2007).
- [40] C. Krellner, T. Förster, H. Jeevan, C. Geibel, and J. Sichelschmidt, *Phys. Rev. Lett.* **100**, 066401 (2008).
- [41] S. Lausberg, A. Hannaske, A. Steppke, L. Steinke, T. Gruner, L. Pedrero, C. Krellner, C. Klingner, M. Brando, C. Geibel, and F. Steglich, *Phys. Rev. Lett.* **110**, 256402 (2013).
- [42] C. Klingner, C. Krellner, M. Brando, C. Geibel, F. Steglich, D. V. Vyalikh, K. Kummer, S. Danzenbächer, S. L. Molodtsov, C. Laubschat, T. Kinoshita, Y. Kato, and T. Muro, *Phys. Rev. B* **83**, 144405 (2011).
- [43] T. Gruner, J. Sichelschmidt, C. Klingner, C. Krellner, C. Geibel, and F. Steglich, *Phys. Rev. B* **85**, 035119 (2012).
- [44] B. K. Rai, M. Stavinoha, J. Banda, D. Hafner, K. A. Benavides, D. A. Sokolov, J. Y. Chan, M. Brando, C.-L. Huang, and E. Morosan, *Phys. Rev. B* **99**, 121109 (2019).
- [45] M. P. Kwasigroch, H. Hu, F. Krüger, and A. G. Green, *Phys. Rev. B* **105**, 224418 (2022).
- [46] We take it to be one half of the difference between the energy of the $N = \infty$ ground state and the $N = \infty, J = 0$ Fermi gas state. For $J\rho \gg 1$, T_K is also precisely the temperature at which the hybridisation field condenses for $N = \infty$ and half-filling.
- [47] Without loss of generality, we have assumed that magnetic order is ferromagnetic. However, since we generally expect $\chi_{ee}(\mathbf{q}) \sim \rho$, in the weak-coupling regime the crossing temperature is similar to the temperature at which magnetic order sets in regardless of the type of order.
- [48] K. Umeo, H. Yamane, H. Kubo, Y. Muro, F. Nakamura, T. Suzuki, T. Takabatake, K. Sengupta, M. K. Forthaus, and M. M. Abd-Elmeguid, *Phys. Rev. B* **85**, 024412 (2012).
- [49] G. Knebel, A. Pourret, S. Rousseau, N. Marquardt, D. Braithwaite, F. Honda, D. Aoki, G. Lapertot, W. Knafo, G. Seyfarth, J.-P. Brison, and J. Flouquet, *Phys. Rev. B* **109**, 155103 (2024).
- [50] D. S. Christovam, M. Sundermann, A. Marino, D. Takegami, J. Falke, P. Dolmantis, M. Harder, H. G. amd Bernhard Keimer, A. Gloskovskii, M. W. Haverkort, I. Elfimov, G. Zwicky, A. V. Andreev, L. Havela, M. M. Bordelon, E. D. Bauer, P. F. S. Rosa, A. Severing, and L. H. Tjeng, (2024), arXiv:2402.03852.
- [51] S. Ran, C. Eckberg, Q.-P. Ding, Y. Furukawa, T. Metz, S. R. Saha, I.-L. Liu, M. Zic, H. Kim, J. Paglione, and N. P. Butch, *Science* **365**, 684 (2019).
- [52] H. Amitsuka, T. Sakakibara, K. Sugiyama, T. Ikeda, Y. Miyako, M. Date, and A. Yamagishi, *Physica B: Condensed Matter* **177**, 173 (1992).
- [53] F. Honda, J. Valenta, J. Prokleška, J. Pospíšil, P. Proschek, J. Prchal, and V. Sechovský, *Phys. Rev. B* **100**, 014401 (2019).

Compound	P (GPa)	x	T_{coh}^* (K)	T_{cross} (K)	$T_{\text{max}}^{\text{hard}}$ (K)	T_N (K)	T_C (K)
UTe ₂ (Ortho.)[15, 16]	0		108 ^{a†}	222	37		
Crossing $b \rightarrow a$	0.6		81 ^{a¶}	184	31		
Metamagnetism observed along b at amb. p.	0.9		65 ^{a¶}	123	24		
	1.1		56 ^{a¶}	108	22		
	1.4		42 ^{a¶}	91	16		
	1.7		28 ^{a¶}	45		3	
UCo _{1-x} Ir _x Ge (Ortho.)[17, 18]		0.00	74 ^a	427 [‡]			2.5
Crossing $b \rightarrow c$		0.02	63 ^a	359 [†]			
Metamagnetism observed for $x > 0.84$ along b		0.07	40 ^a	229			
		0.24	24 ^a	187	35		
		0.40	24 ^a	194	30		
		0.67	15 ^a	45	25		
		0.84	25 ^a	32	13	10.2	
		0.89	31 ^c	27	18	12.2	
		0.92	29 ^c	36	19	14.4	
		1.00	32 ^c	21	29	16.5	
URh _{1-x} Ir _x Ge (Ortho.)[20]		0.00	188 ^a	–			9.5
Crossing $b \rightarrow c$		0.14	–	69 [†]			9.1
Metamagnetism observed along b		0.43	–	–			6.2
		0.45	–	–	~ 11	3.9	
		0.58	–	34	12	7.0	
		1.00	32 ^c	21	29	16.5	
EuCu ₂ (Ge _{1-x} Si _x) ₂ (Tetra.)[19]		0.6	0 [§]	0 [§]		18.8	
Crossing $a \rightarrow b$		0.7	55 ^a	~ 60		15.5	
		0.8	142 ^a	138			
		1.0	300 ^a	> 300?	~ 230		
UIr ₂ Si ₂ (Tetra.)[21]			97 ^c	60	6	5.5	
Crossing $a \rightarrow c$,							
UPt ₂ Si ₂ (Tetra.)[22]			176 ^a	76.5		32	
Crossing $a \rightarrow c$							
Metamagnetism observed along a [52]							
UIrSi ₃ (Tetra.)[23, 53]			224 ^c	93		41.7	
Crossing $a \rightarrow c$							
EuNi ₂ P ₂ (Tetra.)[24]			135 ^a	76	46		
Crossing $ab \rightarrow c$							
Metamagnetism observed along ab							
YbNi ₄ P ₂ (Tetra.)[6, 36, 37]			19 ^c	0.16			0.15
Crossing $\parallel c \rightarrow \perp c$							
CeRuPO (Tetra.)[6, 38–40]			41 ^c	15*			15
Crossing $\perp c \rightarrow \parallel c$							
Yb(Rh _{0.75} Co _{0.25}) ₂ Si ₂ (Tetra.)[6, 41–43]			47 ^c	1.3*			1.3
Crossing $\perp c \rightarrow \parallel c$							
YbIr ₃ Ge ₇ (Rhomb.)[6, 44]			7 ^c	2.9			2.6
Crossing $\parallel c \rightarrow \perp c$							

TABLE I. A table of the coherence temperature T_{coh}^* (K) defined as the maximum in the resistivity; T_{cross} (K), the temperature of the easy axis reorientation; the temperature of the maximum in the low temperature hard axis susceptibility; and T_C (K) or T_N (K) the Curie or Néel temperature for compounds at various doping levels, x , or pressure, P (GPa).

The superscript on T_{coh}^* values indicate the axis for which the resistivity measurement was taken.

* the crossing occurs less than 1 K above the Curie temperature.

† indicates an extrapolation: mCW fits for T_{cross} or linear extrapolation for T_{coh}^* .

‡ the crossing temperature was taken from Ref. [18].

§ No susceptibility crossing or resistivity coherence maximum are observed (this is true for all lower values of x in EuCu₂(Ge_{1-x}Si_x)₂).

¶ The coherence temperatures were determined from linear interpolations of resistivity measurements at different pressure values.